M. J. D. Hayes
Faculty Lecturer
McGill University, Dept. of Mech. Eng. &
Centre for Intelligent Machines,
817 r. Sherbrooke O., Montréal, Québec,
Canada.

M. L. Husty
Associate Professor
Universitätsdozent für Geometrie an der
Montanuniversität Leoben,
Franz-Josef-Straße 18, A-8700 Leoben,
Österreich and
McGill University, Centre for Intelligent
Machines,
817 r. Sherbrooke O., Montréal, Québec,
Canada.

P. J. Zsombor-Murray
Associate Professor
McGill University, Dept. of Mech. Eng. &
Centre for Intelligent Machines,
817 r. Sherbrooke O., Montréal, Québec,
Canada and
Institut für Geometrie, TU Graz,
Kopernikusgasse 24, A-8010 Graz,
Österreich.

Solving the Forward Kinematics of a Planar Three-Legged Platform With Holonomic Higher Pairs

A practical solution procedure for the forward kinematics problem of a fully-parallel planar three-legged platform with holonomic higher pairs is presented. Kinematic mapping is used to represent distinct planar displacements of the end-effector as discrete points in a three dimensional image space. Separate motions of each leg trace skew hyperboloids of one sheet in this space. Therefore, points of intersection of the three hyperboloids represent solutions to the forward kinematics problem. This reduces the problem to solving three simultaneous quadratics. Applications of the platform are discussed and an illustrative numerical example is given.

1 Introduction

1.1 Manipulator Description. The planar manipulator considered in this paper, shown in Fig. 1, consists of three closed kinematic chains. The circular disk, with radius r, rolls without slip on each of the three lines tangent to it. This rolling system is modelled as a pinion meshing with three racks. We call the kinematic connection between a rack and the pinion a gear (G) pair. It is a higher kinematic pair because of the point (or line) contact between the two links. Moreover, the rolling constraints are holonomic due to the pure rolling condition and because the motion is planar. Hence, the constraint equations can be expressed in terms of displacement, i.e., in integral form. Each of the three legs, A, B and C, connect a rack to a base point via two revolute (R) pairs. Each closed loop is an -R-R-G-G-R-R- kinematic chain. Grounded and floating link lengths in each leg are indicated by l_{1_i} and l_{2_i}, respectively, with $i \in \{A, B, C\}$. The leg links are rigid and a rack is rigidly attached to the disk end of each second link. The R-pairs connecting two links in a leg shall be referred to as knee joints K_A, K_B, K_C, and are constrained to move on circles centred on the three points F_A, F_B, F_C, which are grounded to a fixed rigid base. The position and orientation of the pinion end-effector are described by reference frame E, which has its origin on the disk centre and moves with it. Frame Σ has its origin at the base of leg A and is fixed. In the home-position, shown in Fig. 1, the basis directions of E and Σ are identical.

1.2 Background. In 1965 D. Stewart first suggested the use of platform type manipulators as flight simulators (Stewart, 1965). In subsequent years such manipulators came to be known as Stewart platforms. However, a design for a tire test-stand (Gough, 1956), with the same architecture of a modern flight simulator, virtually identical to that proposed by Stewart, had already been put forward by V. E. Gough and the staff at Cornell nine years earlier. We use the term Stewart-Gough platform (SGP) to correct this historical oversight and are, by no means, the first to do so. It is quickly becoming standard terminology in the literature, see Nielsen and Roth (1996), Husty (1996b), Angeles (1997), and Merlet (1998), for example.

The body of literature is thick with investigation on the kinematic analysis of SGP in general. In particular, the forward kinematics (FK) problem of lower-pair-jointed planar SGP has been given extensive attention. It is established in Hunt (1983) that planar SGP with 3 RRR (or the kinematically equivalent, RPR) legs admit at most six real assembly configurations for a given set of activated joint inputs. General solution procedures using elimination theory to derive a 6th degree univariate polynomial, which leads to all assembly configurations, are to be found in Gosselin and Sefrioui (1991) and Wohlhart (1992). The FK problem is solved for all permutations of three-legged planar lower-pair-jointed SGP in Merlet (1996). The univariate polynomial is again derived in Pennock and Kassner (1992), but the work is extended to include an investigation of the workspace in Pennock and Kassner (1993). Earlier work by Gosselin (1988) provides a useful workspace optimisation scheme for planar, spherical and spatial platform-type parallel manipulators. A detailed enumeration of assembly configurations of planar SGP can be found in Rooney and Earle (1983). Synthesis issues are addressed using a straightforward geometric approach in Shirkhodaie and Soni (1987), while Murray and Pierrot (1998) give an extremely elegant n-position synthesis algorithm, based on quaternions, for the design of planar SGP with three RPR legs.

The literature, however, appears to be all but devoid of work investigating fully-parallel planar SGP whose joints include holonomic higher kinematic pairs. This omission is unfortunate because such platforms offer distinct advantages over their lower-pair-jointed cousins in two respects. First, the locations of the attachment points connecting each of the three legs to

Contributed by the Mechanisms Committee for publication in the JOURNAL OF MECHANICAL DESIGN. Manuscript received Apr. 1997; revised Feb. 1999. Associate Technical Editor: V. Kumar.

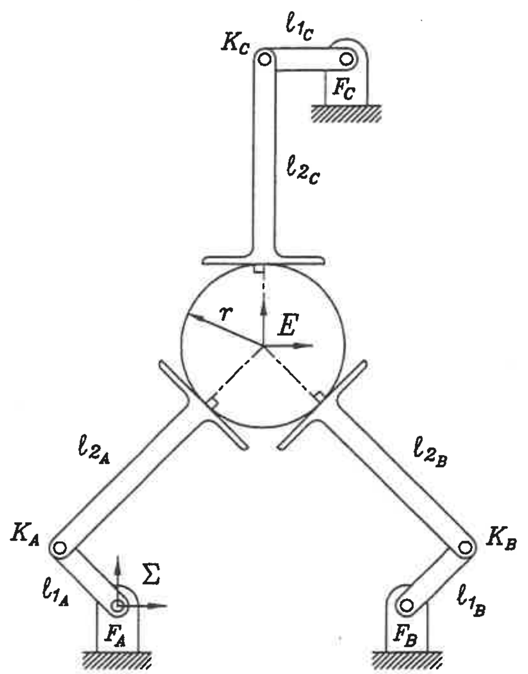

Fig. 1 A planar platform with three DOF

the platform are continuously variable with respect to each other during platform motions, i.e., the platform has a continuously variable geometry. This means that a general procedure for the kinematic analysis of this type of platform can be applied to multiple-arm robots because any such procedure is necessarily dependent on the initial assembly configuration (IAC) of the platform. This leads directly to the second advantage, in that these platforms can be designed as fully parallel, cooperating, or hybrid devices. A good deal of investigation comprises kinematic analysis (Salisbury and Roth, 1983; Hui and Goldenberg, 1989; Mimura and Funahashi, 1992) and control (Cole et al., 1988; Yun et al., 1992) of planar multiple-arm (or, cooperating) robots. Particular attention is given to grasp and its effect on the workspace in Chen and Kumar (1995). The common thread in the multiple arm literature just cited is that the contact between manipulator and object is pure rolling. Grasp and fine-motion manipulation by multi-fingered robotic hands are issues closely connected to contact type. Work in this area is still open, hence we feel justified in examining the kinematic analysis of a three-legged planar SGP with holonomic higher pairs. However, to maintain a reasonable scope for this paper, we will treat the device as a fully-parallel planar manipulator.

It appears that the only work directly related to fully-parallel SGP with holonomic higher pairs comprises the following. The inverse kinematics (IK) problem and workspace of a planar mechanical system comprising a rolling disk manipulated by two 2R legs is investigated in Agrawal and Pandravada (1992, 1993). The IK solution procedure assumes that tangential contact between the arms and disk is maintained during a given motion. Thus, for particular initial and final assembly configurations the mechanical system may be considered as a fully-parallel platform. The analysis, however, is based on a flawed interpretation of the IK problem. The angular measure used to specify the orientation of the disk end-effector must be an absolute quantity in order to have useful meaning in the context of kinematic analysis. Instead, it is defined as the relative angle between normals of the two tangent lines of the manipulating arms. The method, therefore, can not be used for kinematic analysis in any conventional sense. This issue is addressed in Hayes and Zsombor-Murray (1996a), but the IK algorithm presented yields equations that are difficult to solve because they depend on a joint parameter which, it turns out, can not be directly evaluated. A kinematic mapping procedure is used in Hayes and Zsombor-Murray (1996b) to solve the FK problem of a three-legged version of the abovementioned platform, but it assumes a priori knowledge of the platform orientation. This requirement can render the solution procedure somewhat impractical, nevertheless, it was the first step leading directly to the procedure presented herein. It has also led to the first practical IK solution procedure (Hayes and Zsombor-Murray, 1998), which is literally an inverse of the procedure introduced in this paper.

It is important to emphasise that the pure rolling nature of the higher pairs make platforms of the type in Fig. 1 markedly different from lower-pair-jointed SGP. For instance, the pure rolling condition renders FK solutions completely dependent on the IAC (Agrawal and Pandravada, 1992, 1993; Hayes and Zsombor-Murray, 1996b). General planar displacements require a combination of two distinct types of relative rolling with respect to the fixed reference frame: racks roll on the pinion, and the pinion rolls on the racks. There is no obvious way to determine the proportion, which is something that must be done because each type of rolling can produce an identical change in contact point, yet results in an entirely different displacement (Hayes and Zsombor-Murray, 1996a). Moreover, the FK analysis cannot be directly reduced to the lower pair SGP case because of the contact point location ambiguity arising from the rolling constraints. Furthermore, there exists no such equivalent mechanism which can exactly reproduce a rack-and-pinion motion (see Hunt, 1978, p. 106). Methods, such as those discussed in Gosselin and Sefrioui (1991), or Wohlhart (1992), cannot be used until suitably modified to account for the relative rolling. For example, a computational device such as the virtual platform (introduced in section 3.1) must be employed. However, these procedures tend to be poorly suited to this platform type by virtue of the fact that the platform attachment points, i.e., the points of contact between the disk and legs, change relative to each other from pose to pose. This means that many hundreds of coefficients must be computed for every pose. An approach that is independent of the geometry of the contact points would conceivably yield a more elegant procedure.

Recently, it has been shown that kinematic mapping has important applications in planar robot kinematics. A particular mapping (Grünwald, 1911; Blaschke, 1911) is used in De Sa (1979) and De Sa and Roth (1981) to classify one parameter planar algebraic motions. Ravani (1982) and Ravani and Roth (1983) employed it to to study planar motion synthesis. In Husty (1995), the same mapping is utilised in a novel FK solution procedure for planar three-legged SGP. It is then used to analyse the workspace of the same type of platform (Husty, 1996a). The particular mapping used is well suited to manipulators of the type discussed in this paper (see Fig. 1) since it is independent of the geometry of the platform (Husty, 1995). However, it has never, to the best of our knowledge, been applied with complete success to the FK problem of our platform. Indeed, no practical solution procedure can be found in the literature. Thus, the goal of this paper is to present a practical solution procedure, that employs kinematic mapping, for the FK problem of a planar SGP with holonomic higher pairs.

1.3 Applications. The applications of our platform, when considered as a fully-parallel manipulator, are essentially the same as those of regular planar SGP, but the variable platform geometry makes for some interesting additions. For instance, it can be used in situations requiring adjustable, variable coupler length four-bar mechanisms that can be changed to Grashof, change-point, or non-Grashof kinematics. Not only can the coupler curve shape parameters be adjusted, the curve itself can be made uni- or bicursal, to suit the needs of the design at hand. This makes for some welcome flexibility regarding function generation, rigid body guidance and path generation synthesis problems.

Since this is a platform with three degrees-of-freedom (DOF), three motors are required to take full advantage of each DOF. We elect to actuate the three higher pairs. This gives us a measure of control over the relative rolling. The racks are constrained to remain in tangential contact with the pinion. We can maintain passive tangential contact mechanically, see Agrawal and Pandravada (1993) for example. Hence the higher pairs can be activated via a transmission with no additional active joints, eliminating the need for redundant force sensors.

Changing the rack tangent angles changes the assembly configuration of the platform. Each distinct set of inputs yields a distinct set of distances between the knee joints. Referring to Fig. 1, we can lock the racks in two legs so that there is a desired distance between corresponding knee joints. With no loss in generality we can select legs A and B. Since two of the actuators are locked, the platform loses 2 DOF. Furthermore, the ungrounded links in legs A and B, together with the pinion are a temporary rigid body with an effective length corresponding to the distance between the two knee joints, K_A and K_B. The resulting four-bar mechanism can be driven with rack C. If the link lengths are suitably chosen, it will be a convertible Grashof-Change-Point-Non-Grashof mechanism.

Figure 2 illustrates the most general situation, where the grounded links in legs A and B have different lengths. Cases (i) through (iii) show the mechanisms that result as the effective coupler length, given in generic units, varies between 15, 14, and 12. The sum of the longest (l) and shortest (s) link lengths is less than, equal to, and greater than the sum of the other two (a and b) giving Grashof, change-point, and non-Grashof mechanisms, respectively. Recall the characteristics of these three variants of a four-bar mechanism. As a reminder, the excursion arcs and singular positions of the small and large arm crank pins for each of the three cases are shown on the right. For this application the link lengths in the driving leg, C, and the disk radius are unimportant provided they allow for the desired coupler lengths and output error tolerance.

2 A Kinematic Mapping of Planar Displacements

We now briefly describe the kinematic mapping used in this paper. Very detailed accounts may be found in De Sa (1979), Ravani (1982), Bottema and Roth (1990). It was introduced in 1911 simultaneously, and independently, by Grünwald (1911) and Blaschke (1911). We begin by observing that a general displacement in the plane requires three independent parameters to fully characterise it. It is convenient to think of the relative planar motion between two rigid bodies as the motion of a Cartesian reference coordinate system E attached to one of the bodies, with respect to the Cartesian coordinate system Σ attached to the other. Without loss of generality, Σ may be considered as fixed while E is free to move. Then the position of a point in E relative to Σ can be given by the homogeneous linear transformation

$$\begin{bmatrix} X \\ Y \\ Z \end{bmatrix} = \begin{bmatrix} \cos\varphi & -\sin\varphi & a \\ \sin\varphi & \cos\varphi & b \\ 0 & 0 & 1 \end{bmatrix} \begin{bmatrix} x \\ y \\ z \end{bmatrix}, \qquad (1)$$

where the ratios $(x : y : z)$ represent the homogeneous coordinates of a point in E, while $(X : Y : Z)$ are those of the same point in Σ. The Cartesian coordinates of the origin of E measured in Σ are (a, b), while φ is the rotation angle measured from the X-axis to the x-axis, the positive sense being counter-clockwise. Clearly, in Eq. (1) the three characteristic displacement parameters are (a, b, φ).

Any planar displacement can be expressed as the product of isometries in many ways. In particular, as two reflections whose mirror lines intersect in a point (Coxeter, 1969). That is, a single rotation, through twice the angle between the mirrors, about the point of intersection. This is also true for the product of two parallel translations, except the corresponding two parallel mirrors, separated by one half the magnitude of the combined translation, intersect in a point on the line at infinity, and the rotation angle is infinitesimal. The homogeneous coordinates of the rotation centre, $(X_p : Y_p : Z_p)$, are called the pole of the displacement. The coordinates of the pole are the same in both E and Σ and are therefore invariant, i.e., $(X_p : Y_p : Z_p) = (x_p : y_p : z_p)$. The pole coordinates of any displacement can be expressed in terms of the displacement parameters, (a, b, φ), and thus convey sufficient information to characterise it.

To obtain the pole coordinates in terms of (a, b, φ) we first determine the linear algebraic invariants of a general planar displacement (Salmon, 1885). They are found by determining the eigenvalues of the 3×3 transformation matrix in Eq. (1), which are

$$\lambda_1 = 1,$$
$$\lambda_{2,3} = e^{\pm i\varphi}.$$

There is only one real eigenvalue and it is the same for all displacements. The homogeneous components of the eigenvector that corresponds to the real eigenvalue yield the desired expression for the invariant pole coordinates:

$$\begin{bmatrix} X_p \\ Y_p \\ Z_p \end{bmatrix} = \begin{bmatrix} x_p \\ y_p \\ z_p \end{bmatrix} = \frac{1}{2}\begin{bmatrix} a - b\tan(\varphi/2) \\ a\tan(\varphi/2) + b \\ 2 \end{bmatrix}. \qquad (2)$$

The validity of this fact is confirmed by substituting Eq. (2) into Eq. (1). If k is a real non-zero quantity then $(x : y : z)$ and $k(x : y : z)$ represent the same point in the real projective plane (Coxeter, 1969). Without loss in generality, we may let $k = 2\sin(\varphi/2)$, and multiply the pole coordinates to obtain

$$\begin{bmatrix} X_p \\ Y_p \\ Z_p \end{bmatrix} = \begin{bmatrix} x_p \\ y_p \\ z_p \end{bmatrix} = \begin{bmatrix} a\sin(\varphi/2) - b\cos(\varphi/2) \\ a\cos(\varphi/2) + b\sin(\varphi/2) \\ 2\sin(\varphi/2) \end{bmatrix}. \qquad (3)$$

Many mappings can be defined that take a triple of planar displacement parameters (a, b, φ) in the moving coordinate

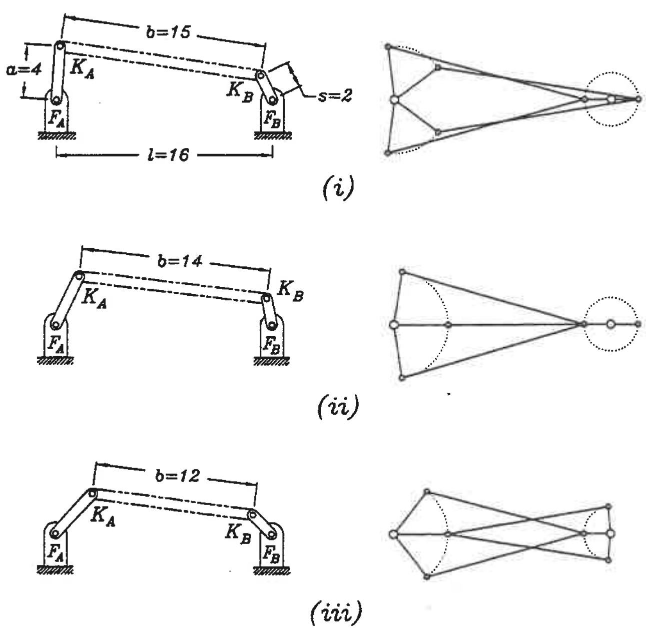

Fig. 2 Application to planar four-bar mechanisms: (i) Grashof; (ii) change-point; (iii) non-Grashof

system E, with respect to the fixed system Σ, to a point described by the homogeneous coordinates $(X_1 : X_2 : X_3 : X_4)$ of a three dimensional projective image space, Σ'. The mapping used here takes a displacement pole, given by the homogeneous point coordinates $(X_p : Y_p : Z_p)$, to an image point in Σ'. It is defined as:

$$(X_1 : X_2 : X_3 : X_4) = (X_p : Y_p : Z_p : \tau Z_p), \tag{4}$$

where

$$\tau = \cot(\varphi/2),$$
$$0 < \varphi \leq 2\pi.$$

Thus, the image point, in terms of the displacement parameters (a, b, φ), is

$$(X_1 : X_2 : X_3 : X_4) = [(a \sin(\varphi/2) - b \cos(\varphi/2) : (a \cos(\varphi/2) + b \sin(\varphi/2) : 2 \sin(\varphi/2) : 2 \cos(\varphi/2)]. \tag{5}$$

The algebraic construction of the mapping requires the multiplication of Z_p by cot $\varphi/2$. Of course, cot $\varphi/2$ is not defined when $\varphi = 0$, and vanishes when $\varphi = 2\pi$. For the purpose of constructing $X_4 = \tau Z_p$, we impose the limits $0 < \varphi \leq 2\pi$. After this multiplication has been made, we have $X_4 = 2 \cos \varphi/2$. Now we can allow φ to take on any value, mod (2π), because cos $\varphi/2$ is defined for all real values of φ. Hence all distinct displacements have unique image points: the identity displacement is the point $(0 : 0 : 0 : 1)$; pure translations, given by triples $(a, b, 0)$, and half-turns, given by triples (a, b, π), map onto the points in the planes $X_3 = 0$ and $X_4 = 0$, respectively.

By virtue of the relationships expressed in Eq. (5), the transformation matrix from Eq. (1) may be expressed in terms of the homogeneous coordinates of the image space, Σ'. This means that we now have a linear transformation to express a displacement of E with respect to Σ in terms of the image point:

$$\begin{bmatrix} X \\ Y \\ Z \end{bmatrix} = \begin{bmatrix} (X_4^2 - X_3^2) & -2X_3X_4 & 2(X_1X_3 + X_2X_4) \\ 2X_3X_4 & (X_4^2 - X_3^2) & 2(X_2X_3 - X_1X_4) \\ 0 & 0 & (X_4^2 + X_3^2) \end{bmatrix} \begin{bmatrix} x \\ y \\ z \end{bmatrix}. \tag{6}$$

Since each distinct displacement described by (a, b, φ) has a corresponding unique image point, the inverse mapping can be obtained from Eq. (5): for a given point of the image space, the displacement parameters are

$$\tan(\varphi/2) = X_3/X_4,$$
$$a = 2(X_1X_3 + X_2X_4)/(X_3^2 + X_4^2),$$
$$b = 2(X_2X_3 - X_1X_4)/(X_3^2 + X_4^2). \tag{7}$$

Equations (7) give correct results when either X_3 or X_4 is zero. Caution is in order, however, because the mapping is injective, not bijective: there is at most one pre-image for each image point. Thus, not every point in the image space represents a displacement. It is easy to see that any image point on the real line $X_3 = X_4 = 0$ has no pre-image and therefore does not correspond to a real displacement of E. From Eq. (7), this condition renders φ indeterminate and places a and b on the line at infinity.

We will now derive the required image space constraint equation. The ungrounded R-pair in a 2R mechanism is forced to move on a circle with a fixed centre. The image points that correspond to all possible displacements of the ungrounded link, with respect to a fixed reference frame, constitute a quadric hyper-surface (Bottema and Roth, 1990). It's expression can be obtained in the following way: the equation of a circle with

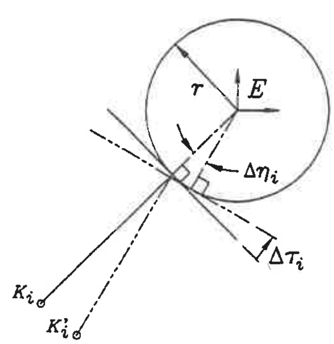

Fig. 3 If tangential contact is maintained $\Delta\tau_i = \Delta\eta_i$

radius r centred on the homogeneous coordinates $(X_c : Y_c : Z)$ has the form

$$(X - X_cZ)^2 + (Y - Y_cZ)^2 - r^2Z^2 = 0. \tag{8}$$

Expanded, this becomes

$$X^2 + Y^2 - 2XX_cZ - 2YY_cZ + X_c^2Z^2 + Y_c^2Z^2 - r^2Z^2 = 0. \tag{9}$$

Setting

$$C_1 = -X_c,$$
$$C_2 = -Y_c,$$
$$C_3 = (C_1^2 + C_2^2 - r^2) = (X_c^2 + Y_c^2 - r^2),$$

yields

$$X^2 + Y^2 + 2C_1XZ + 2C_2YZ + C_3Z^2 = 0. \tag{10}$$

Substituting the expressions for X, Y, Z from Eq. (6) into Eq. (10) produces the following quadric:

$$\begin{aligned} H : 0 = {} & z^2(X_1^2 + X_2^2) + (1/4)[(x^2 + y^2) - 2C_1xz \\ & - 2C_2yz + C_3z^2]X_3^2 + (1/4)[(x^2 + y^2) + 2C_1xz \\ & + 2C_2yz + C_3z^2]X_4^2 + (C_1z - x)zX_1X_3 \\ & + (C_2z - y)zX_2X_3 - (y + C_2z)zX_1X_4 \\ & + (C_1z + x)zX_2X_4 + (C_2x - C_1y)zX_3X_4. \end{aligned} \tag{11}$$

The projection of this quadric hyper-surface in the (X_1, X_2, X_3) sub-space, determined by $X_4 = 1$, is a skew hyperboloid. Its trace in the plane X_3 = constant is a circle. The points on any of these circles represent translations of the disk with a fixed orientation.

3 An Application to the FK Problem

The FK problem is conventionally expressed as a transformation of the position and orientation of the end effector from a joint space representation to a Cartesian space representation. In other words, given a set of n joint variables, one per degree-of-freedom, determine the position and orientation of the end effector with respect to a non-moving reference coordinate system. Since the platform has three DOF, three joint input variables are required. As previously mentioned, we select the three joint input variables to be the change in arclength, measured along each of the three racks, due to the change in contact points. They are given by the three numbers $\Delta d_i = r\Delta\tau_i$, $i \in \{A, B, C\}$, where the Δd_i are the changes in arclength, the radius of the pinion is r, and the $\Delta\tau_i$ are the change between the initial and final rack angles. The $\Delta\tau_i$ also represent the change in angle of the disk tangents because tangential contact is maintained between each rack and the pinion. The Δd_i and $\Delta\tau_i$ are coordinate reference frame independent because they are differences. Furthermore, since the bases are orthogonal, the change in tangent angle is the same as the change normal angle, $\Delta\eta_i$. This is illustrated in Fig. 3.

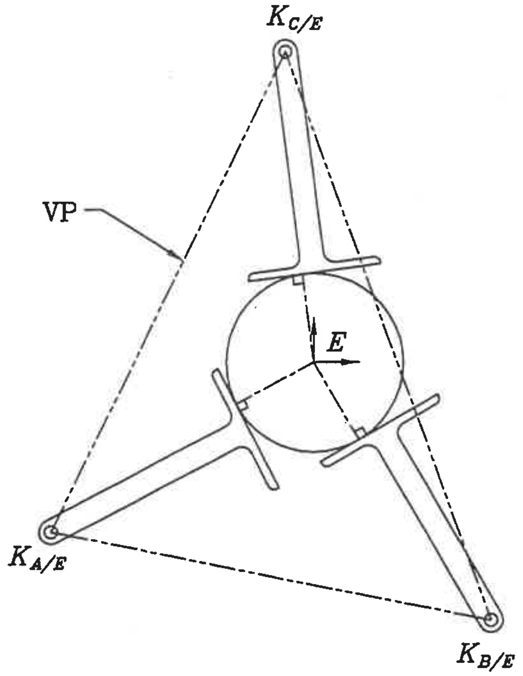

Fig. 4 The VP for a given set of inputs

3.1 Virtual Platform. Solving the FK problem for our manipulator, with Husty's procedure (Husty, 1995), requires platform points with fixed positions in the moving frame E which move on circles in the non-moving frame Σ. In order to establish these points we must first define the platform (or end-effector). The only points bound to move on circles in Σ are points on the first link in each leg, which are connected to the fixed base by an R-pair. We will use the revolute centres of the three knee joints, K_A, K_B and K_C. Now, consider a virtual platform (VP) formed by the triangle whose vertices are the three knee joints expressed relative to the disk frame E: $K_{A/E}$, $K_{B/E}$, $K_{C/E}$ (see Fig. 4). We call these vertices virtual platform points (VPP). For a given assembly configuration, the VPP are fixed relative to each other, but change from pose to pose. In turn, this means the VP geometry changes continuously during platform motion. However, for any given displacement it can be considered a rigid body, since we are only interested in the correspondence between an initial and a final position. Hence, the VPP meet the requirements of being fixed points in E which move on circles in Σ.

3.2 Involute Inputs. The next task is to develop expressions for the VPP so they can be used as inputs to the kinematic mapping. We want the VPP in terms of the joint input variables. Consider, for now, only leg A in Fig. 5 and observe that the knee joint K_A has a fixed position in the reference frame attached to the rack, R_A. We know it moves on a circle in Σ, but it also experiences motion relative to the moving disk frame E. What is required is a description of that motion in terms of the joint inputs. This turns out to be straightforward: fix the disk and notice that the relative motion of the rack with respect to E is pure rolling with the original contact point moving on an involute of the pinion. There is a bijective correspondence, that depends on the change in rack tangent angle, between positions of a given rack point on its involute and knee joint positions. This gives a complete description of the motion of the knee joints in terms of the input variables. Due to their positional dependence on an involute, we call these one parameter sets of knee joint positions involute inputs.

The motion of the knee joints of the remaining two legs must be the same type as that of leg A relative to E, but the starting points of the involutes are different. Thus, for every set of three joint input parameters one obtains a set of three VPP expressed in E. With the VPP transformed as involute inputs the kinematic mapping can be used.

In what follows, we will show how the involute inputs can be derived. Figure 5 shows the reference coordinate systems used to transform the position of the knee joint K_A from the moving rack reference frame, R_A, to the relatively fixed pinion reference frame, E. The origin of R_A moves along its involute and R'_A gives the new position of R_A after a change in tangent angle, $\Delta\tau_A$. The intermediate system accounting for the location of the starting point and orientation of the involute, E'_A, is fixed relative to E. Examining Fig. 5, it is easy to see that for each leg the required transformation to take the coordinates of the knee joint K_i from frame R'_i to frame E are the concatenation of transformations expressing points in frame R'_i relative to frame E'_i and those expressing points in frame E'_i relative to frame E:

$$\mathbf{T}_{R'_i/E} = \mathbf{T}_{E'_i/E}\mathbf{T}_{R'_i/E'_i} = \begin{bmatrix} c\theta_i & -s\theta_i & 0 \\ s\theta_i & c\theta_i & 0 \\ 0 & 0 & 1 \end{bmatrix}$$

$$\times \begin{bmatrix} -s\Delta\tau_i & -c\Delta\tau_i & r(c\Delta\tau_i + \Delta\tau_i s\Delta\tau_i) \\ c\Delta\tau_i & -s\Delta\tau_i & r(s\Delta\tau_i - \Delta\tau_i c\Delta\tau_i) \\ 0 & 0 & 1 \end{bmatrix},$$

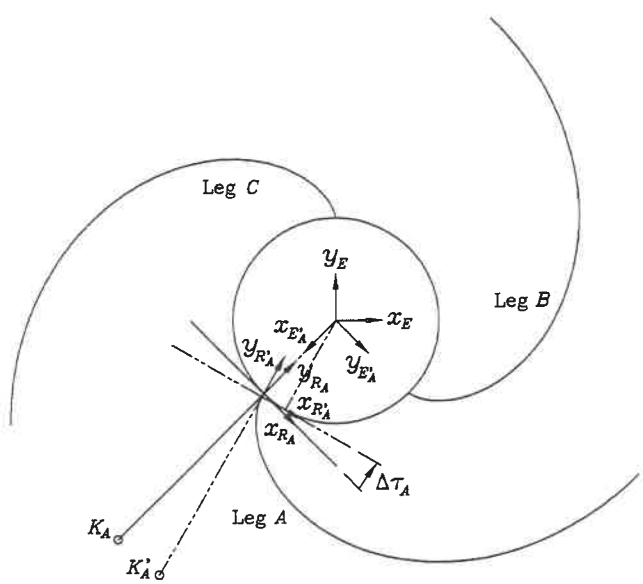

Fig. 5 Reference systems in leg A after a rotation $\Delta\tau_A$

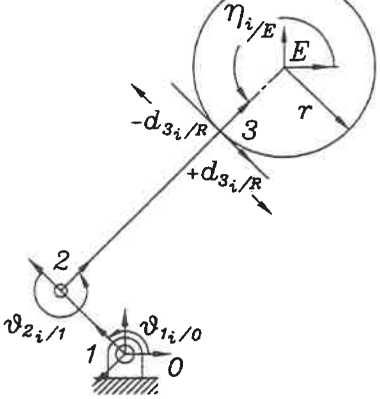

Fig. 6 Reference frames and parameters for the i_{th} leg

Table 1 Fixed base points in Σ, joint inputs, and VPP

i	$x_{0_i/\Sigma}$	$y_{0_i/\Sigma}$	$\Delta\tau_i$	$x_{K_i/E}$	$y_{K_i/E}$
A	0	0	$-17.5°$	-11.85401931	-7.548168766
B	$10\sqrt{2}$	0	$-15°$	7.906899696	-11.60075686
C	$5\sqrt{2}+4$	$9\sqrt{2}+14$	7.5°	-1.308247378	13.94857141

where $c \equiv \cos$, and $s \equiv \sin$.

The geometrical significance of $\mathbf{T}_{R_i'/E_i'}$ is seen when each column is examined. The first column is the direction of the disk tangent in E_i' (the direction of the x-axis of frame R_i'). The second column is the direction in E_i', towards the centre of the pinion, of the normal at the new contact point (the direction of the y-axis of frame R_i'). The third column is the position of the origin of frame R_i' on the involute, also expressed in E_i'. The remaining transformation, $\mathbf{T}_{E_i'/E}$, depends on the angle between the x-axis of frame E and the rack normal in the home-position.

The knee joints, shown in Fig. 1, all have the same coordinates in their respective R_i frames:

$$\mathbf{k}_{i/R_i} = \mathbf{k}_{i/R_i'} = \begin{bmatrix} 0 \\ -l_{2_i} \\ 1 \end{bmatrix}.$$

Once the changes in rack tangent angle (joint inputs), $\Delta\tau_i$, are specified the coordinates of the knee joints (involute inputs) in frame E, $\mathbf{k}_{i/E}$, are easily determined by left multiplying the $\mathbf{k}_{i/R_i'}$ with the appropriate $\mathbf{T}_{R_i'/E}$,

$$\mathbf{k}_{i/E} = \mathbf{T}_{R_i'/E}\mathbf{k}_{i/R_i'}. \quad (12)$$

3.3 FK Solution Procedure. To obtain the solutions for a given set of inputs, begin by removing the VP connections with legs B and C. That is, consider only the open kinematic chain consisting of the base, F_A, the first link, l_{1_A}, and the VP described by positions of the three knee joints in frame E, $K_{i/E}$, $i \in \{A, B, C\}$. Observe that the higher pairs are locked in the corresponding VP configuration by virtue of the specified input parameters. There can be no relative motion between the disk and the rack because that would change the relative positions of the VPP. Knee joint K_A is constrained to move on a circle with centre F_A and radius l_{1_A} (see Fig. 1). Furthermore, the VP can rotate about K_A. The kinematic image of this set of two parameter displacements is the two parameter constraint hyperboloid, H_A, given by Eq. (11). All poses of this virtual rigid body correspond to the image points on H_A.

When the other two VP connection points (K_B and K_C) are analysed in turn, two additional hyperboloidal constraint surfaces are generated, H_B and H_C. The points on each hyperboloid correspond to the complete range of possible displacements around the points still connected. The points of intersection of H_A, H_B and H_C represent the positions of the VP where its three knee joints are on their respective circles. Therefore, these points of intersection constitute the solution(s) to the FK problem. Three distinct quadrics can have, at most, eight real intersections. However, it is shown in Bottema and Roth (1990) that all such constraint hyperboloids contain the points $J_1(1 : i : 0 : 0)$ and $J_2(1 : -i : 0 : 0)$. These two points are, therefore, always in the solution set and must be discarded because they are on the line $X_3 = X_4 = 0$ and hence correspond to no real displacement. Thus, there are a maximum of six real solutions to the FK problem for manipulators of this type, which confirms the well known result established in Hunt (1983).

4 Example

Table 1 gives the coordinates of the base points F_A, F_B, F_C in the fixed frame Σ with origin at F_A, the change in rack tangent angles, and the corresponding knee joint positions in E (the VPP), given by Eq. (12). The link lengths, in generic units, are: $r = 4$, $l_{1_i} = 4$, $l_{2_i} = 10$, the reference angles between E_i' and E in the home-position are $\theta_i = (225$ deg, 315 deg, 90 deg), and the IAC are $(\eta_{i/E})_{\text{initial}} = (225$ deg, 315 deg, 90 deg), $(d_{3_i/R})_{\text{initial}} = (0, 0, 0)$, $(\vartheta_{1_i/0})_{\text{initial}} = (135$ deg, 45 deg, 180 deg), and $(\vartheta_{2_i/1})_{\text{initial}} = (270$ deg, 90 deg, 90 deg), where $i \in \{A, B, C\}$. The link reference frames (0, 1, 2, 3, etc.) were assigned using the Denavit-Hartenberg convention (Angeles, 1998). Figure 6 shows those of the i^{th} leg.

Setting $z = 1$ in Eq. (11), which can always be done as no practical VP will have a vertex on the line at infinity $(x : y : 0)$, and then substituting the VPP from Table 1 into Eq. (11) determines the three constraint hyperboloids. X_4 is used as the

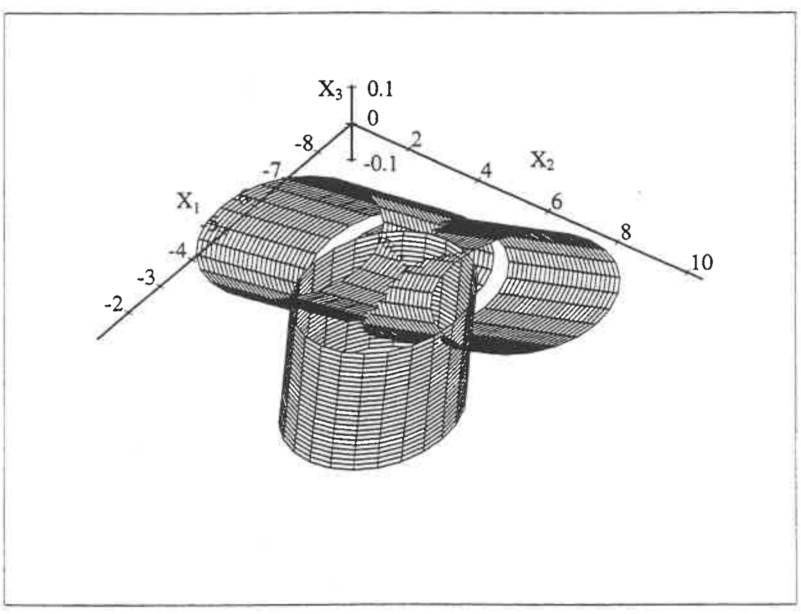

Fig. 7 The constraint hyperboloids in the $X_4 = 1$ projection of the image space

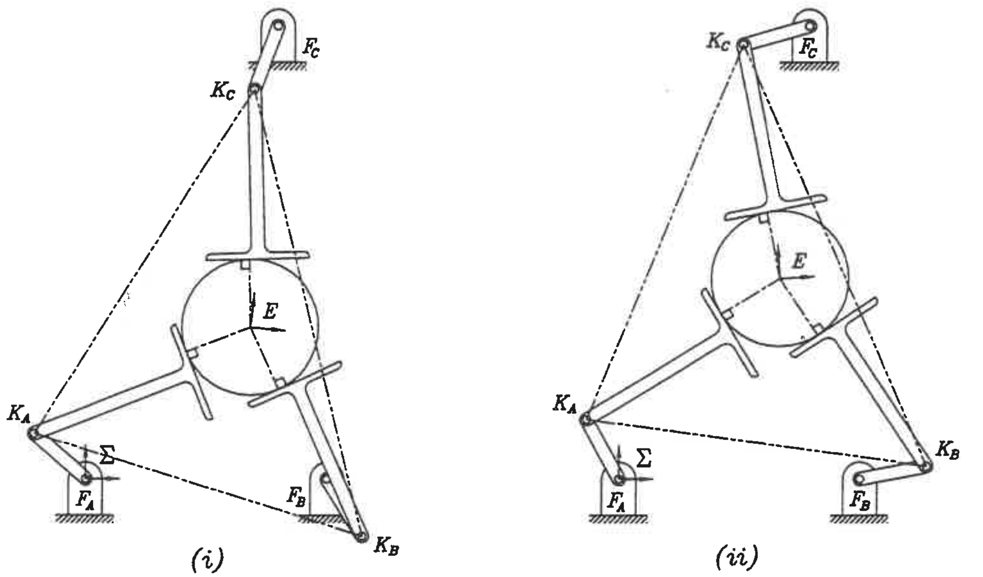

Fig. 8 The two real solutions: (*i*) solution 1; (*ii*) solution 2

homogenising coordinate in the image space, hence $X_4 = 0$ represents the plane at infinity, but also corresponds to VP rotations of $\varphi = 180$ deg. Therefore, $X_4 = 0$ is a practical concern, unlike the case of $z = 0$. However, this condition gives only one pair of solutions for all sets of three constraint hyperboloids, namely J_1 and J_2. This being the case, we can safely normalise the image space homogeneous coordinates, setting $X_4 = 1$, by multiplying $(X_1 : X_2 : X_3 : X_4)$ through by $(1/2) \sec \varphi/2$. Solving the resulting set of three equations, $H_A = 0$, $H_B = 0$, $H_C = 0$, for X_1, X_2, X_3 gives two real and two pairs of complex conjugate solutions. The two real solutions are:

$$S_1: \quad X_1 = -4.724652386, X_2 = 4.561069802, \quad X_3 = -0.05146192114,$$

$$S_2: \quad X_1 = -5.754360118, X_2 = 4.906081896, \quad X_3 = 0.03244152899.$$

The solution set always contains an even number of real solutions because those that are complex arise in conjugate pairs. Figure 7 is a view, projected into the sub-space induced by $X_4 = 1$, of the resulting hyperboloids showing one of the intersections. The position and orientation of the disk corresponding to each real solution in terms of the displacement parameters (a, b, φ) can be found by substituting the values for X_1, X_2, X_3, along with $X_4 = 1$ into the set of Eqs. (7). The resulting pair of real displacement parameters are given in Table 2.

The rack tangent angle inputs, $\Delta\tau_i$, in Table 1, expressed relative to the disk frame E, reveal the geometry of the VP. The origin of E is on the disk centre. Once the orientation and position of the VP, and hence E, are obtained as a triple of displacement parameters (a, b, φ), it is a simple matter of plane trigonometry to determine the relative link angles for the assembly configuration that correspond to the solution. Figure 8 illustrates the two real assembly configurations, where the vertices of the VP are on their respective circles.

Table 2 Displacement parameters

Solution	a	b	φ (deg.)
1	9.583039940	8.956143130	−5.891904208
2	9.428879858	11.81460751	3.716222033

5 Conclusions

A practical solution procedure for the FK problem of platforms of the type in Fig. 1 has been presented. In it, kinematic mapping has proven to be a useful tool. The involute inputs to the mapping are the knee joint positions expressed as one parameter displacements of initial rack contact points along involutes of the disk. Once the VP is established, conventional solution procedures can be used, however they are generally poorly suited to the task. The reason for this is due to the presence of higher kinematic pairs and the variable platform geometry they induce. The kinematic mapping procedure is preferable because it is independent of the platform geometry, and the rolling contacts are rendered innocuous because they can be embedded in the inputs. In the example, only two real solutions were found. However, there can be as many as six, always arising in pairs. This solution is fundamental to any further investigation of this type of platform, which is worth while because of the applications it can add to repertoire of planar SGP.

6 Acknowledgments

The authors gratefully acknowledge the financial support provided by research grants from the Natural Sciences & Engineering Research Council of Canada (NSERC) and le Fonds pour la Formation des Chercheurs et l'aide à la Reserche (FCAR) of the Province of Québec.

References

1 Agrawal, S. K., and Pandravada, R., 1992, "Inverse Kinematic Solutions of a Rolling Disk Between Two Planar Manipulators," *Robotics, Spatial Mechanisms, and Mechanical Systems*, ASME, DE-Vol. 45, pp. 473–478.

2 Agrawal, S. K., and Pandravada, R., 1993, "Kinematics and Workspace of a Rolling Disk Between Planar Manipulators," *Proc. Am. Control Conf.*, San Francisco, CA, pp. 741–745.

3 Angeles, J., 1997, *Fundamentals of Robotic Mechanical Systems: Theory, Methods, and Algorithms*, Springer-Verlag, New York, N.Y., p. 318.

4 Blaschke, W., 1911, "Euklidische Kinematik und nichteuklidische Geometrie," *Zeitschr. Math. Phys.*, Vol. 60, pp. 61–91 and 203–204.

5 Bottema, O., and Roth, B., 1990, *Theoretical Kinematics*, (originally published in 1979 by North-Holland Publishing Co., Amsterdam, as Vol. 24 of North-Holland Series in Applied Mathematics and Mechanics) Dover Publications, Inc., New York, N.Y.

6 Chen, W., and Kumar, V., 1995, "Workspace of Planar Cooperating Robots with Rolling Contacts," *Advanced Robotics*, The Int'l J. of the Robotics Soc. of Japan, Vol. 9, No. 5, pp. 483–504.

7 Cole, A., Hauser, J., and Sastry, S., 1988, "Kinematics and Control of Multifingered Hands with Rolling Contact," *Proc. of IEEE Int. Conf. on Rob. and Aut.*, pp. 228–233.

8 Coxeter, H. S. M., 1969, *Introduction to Geometry,* second edition, John Wiley & Sons, Inc., Toronto, Ont., Canada.
9 De Sa, S., 1979, "Classification and Properties of Planar Motion Using Kinematic Mappings," Dissertation, Stanford University, Stanford, CA.
10 De Sa, S., Roth, B., 1981, "Kinematic Mappings. Part 1: Classification of Algebraic Motions in the Plane," ASME, *J. of Mech. Design,* Vol. 103, pp. 585–591.
11 Gosselin, C., 1988, "Kinematic Analysis, Optimization and Programming of Parallel Robotic Manipulators," Ph.D. thesis, Dept. of Mech. Eng., McGill University, Montréal, Qué, Canada.
12 Gosselin, C., and Sefrioui, J., 1991, "Polynomial Solutions for the Direct Kinematics Problem of Planar Parallel Three-Degree-of-Freedom Parallel Manipulators," *Proc. 5th Int. Conf. on Adv. Rob.* (ICAR), Pisa, Italy, pp. 1124–1129.
13 Gough, V. E., 1956, "Discussion in London: Automobile Stability, Control, and Tyre Performance," *Proc. Automobile Division, Institution of Mech. Engrs.,* pp. 392–394.
14 Grünwald, J., 1911, "Ein Abbildungsprinzip, welches die ebene Geometrie und Kinematik mit der räumlichen Geometrie verknüpft," *Sitzber. Ak. Wiss. Wien,* Vol. 120, pp. 677–741.
15 Hayes, M. J. D., Zsombor-Murray, P. J., 1996a, "A Planar Parallel Manipulator with Holonomic Higher Pairs: Inverse Kinematics," *Proc. CSME Forum 1996, Symposium on the Theory of Machines and Mechanisms,* Hamilton, Ont., Canada, pp. 109–116.
16 Hayes, M. J. D., Zsombor-Murray, P., 1996b, "Kinematic Mapping of 3-legged Planar Platforms With Holonomic Higher Pairs," *Recent Advances in Robotic Kinematics,* eds. Lenarčič, J., Parenti-Castelli, V., Kluwer Academic Publishers, Dordrecht, pp. 421–430.
17 Hayes, M. J. D., and Zsombor-Murray, P., 1998, "Inverse Kinematics of a Planar Manipulator with Holonomic Higher Pairs," *Recent Advances in Robotic Kinematics,* eds. Lenarčič, Husty, M. L., Kluwer Academic Publishers, Dordrecht, pp. 59–68.
18 Hui, R., and Goldenberg, A. A., 1989, "Formulation of the Hybrid Control Architecture Using the Constrained Manipulator Model-Application to Rolling Manipulation of a Rigid Object Using a Dextrous Robotic Hand," *Second Workshop on Military Robotic Applications,* Kingston, Ont., Canada, pp. 316–323.
19 Hunt, K. H., 1978, *Kinematic Geometry of Mechanisms,* Clarendon Press, Oxford, England.
20 Hunt, K. H., 1983, "Structural Kinematics of In-Parallel-Actuated Robot Arms," *ASME J. of Mech., Trans. and Automation in Design,* Vol. 105, No. 4, pp. 705–712.
21 Husty, M. L., 1995, "Kinematic Mapping of Planar Three-Legged Platforms," *Proc. 15th Canadian Congress of Applied Mechanics,* CANCAM 1995, Vol. 2, pp. 876–877.
22 Husty, M. L., 1996a, "On The Workspace of Planar Three-legged Platforms," *Proc. World Automation Conf., 6th Int. Symposium on Rob. and Manuf.* (ISRAM 1996), Montpellier, France, Vol. 3, pp. 339–344.
23 Husty, M. L., 1996b, "An Algorithm for Solving the Direct Kinematics of General Stewart-Gough Platforms," *Mechanism and Machine Theory,* Vol. 31, No. 4, pp. 365–379.
24 Merlet, J-P., 1996, "Direct Kinematics of Planar Parallel Manipulators," *IEEE Int. Conf. on Robotics and Automation,* Minneapolis, MN, pp. 3744–3749.
25 Merlet, J-P., 1998, "Determination of the Presence of Singularities in 6-D Workspace of a Gough Parallel Manipulator," *Advances in Robot Kinematics: Analysis and Control,* eds. Lenarčič, J., Husty, M. L., Kluwer Academic Publishers, Dordrecht, pp. 39–48.
26 Mimura, N., and Funahashi, Y., 1992, "Kinematics of Planar Multifingered Robot Hand with Displacement of Contact Points," *JSME International Journal,* Series 3, Vol. 35, No. 3, pp. 462–469.
27 Murray, A. P., Pierrot, F., 1998, "N-Position Synthesis of Parallel Planar RPR Platforms," *Advances in Robot Kinematics: Analysis and Control,* eds. Lenarčič, J., Husty, M. L., Kluwer Academic Publishers, Dordrecht, pp. 69–78.
28 Nielsen, J., and Roth, B., 1996, "The Direct Kinematics of the General 6-5 Stewart-Gough Mechanism," *Recent Advances in Robotic Kinematics,* eds. Lenarčič, J., Parenti-Castelli, V., Kluwer Academic Publishers, Dordrecht, pp. 7–16.
29 Pennock, G. R., and Kassner, D. J., 1992, "Kinematic Analysis of a Planar Eight-Bar Linkage: Application to a Platform-Type Robot," ASME JOURNAL OF MECHANICAL DESIGN, Vol. 114, No. 1, pp. 87–95.
30 Pennock, G. R., and Kassner, D. J., 1993, "The Workspace of a General Geometry Planar Three-Degree-of-Freedom Platform-Type Manipulator," ASME JOURNAL OF MECHANICAL DESIGN, Vol. 115, pp. 269–276.
31 Ravani, B., 1982, "Kinematic Mappings as Applied to Motion Approximation and Mechanism Synthesis," Dissertation, Stanford University, Stanford, CA.
32 Ravani, B., and Roth, B., 1983, "Motion Synthesis Using Kinematic Mappings," ASME *Journal of Mechanisms, Transmissions, & Automation in Design,* Vol. 105, pp. 460–467.
33 Rooney, J., and Earle, C. F., 1983, "Manipulator Postures and Kinematics Assembly Configurations," *6th World Congress on Theory of Machines and Mechanisms,* New Delhi, pp. 1014–1020.
34 Salisbury, J. K., and Roth, B., 1983, "Kinematic and Force Analysis of Articulated Mechanical Hands," ASME *Journal of Mechanical Transmissions and Automation in Design,* Vol. 105, pp. 35–41.
35 Salmon, G., 1885, *Lessons Introductory to the Modern Higher Algebra,* fourth edition, Hodges, Foster, and Figgis, Dublin, Ireland.
36 Shirkhodaie, A. H., and Soni, A. H., 1987, "Forward and Inverse Synthesis for a Robot with Three Degrees of Freedom," *19th Summer Computation Simulation Conference,* Montréal, Québec, Canada, pp. 851–856.
37 Stewart, D., 1965, "A Platform With Six Degrees of Freedom," *Proc. Institution of Mech. Engrs.,* Vol. 180, Part 1, No. 15, pp. 371–378.
38 Wohlhart, K., 1992, "Direct Kinematic Solution of the General Planar Stewart Platform," *Proc. of the Int. Conf. on Comp. Int. Manu.,* Zakopane, pp. 403–411.
39 Yun, X., Kumar, V., Sarkar, N., Paljug, E., 1992, "Control of Multiple Arms with Rolling Constraints," *Proc. of IEEE Int. Conf. Rob. Aut.,* Nice, France, pp. 2193–2198.